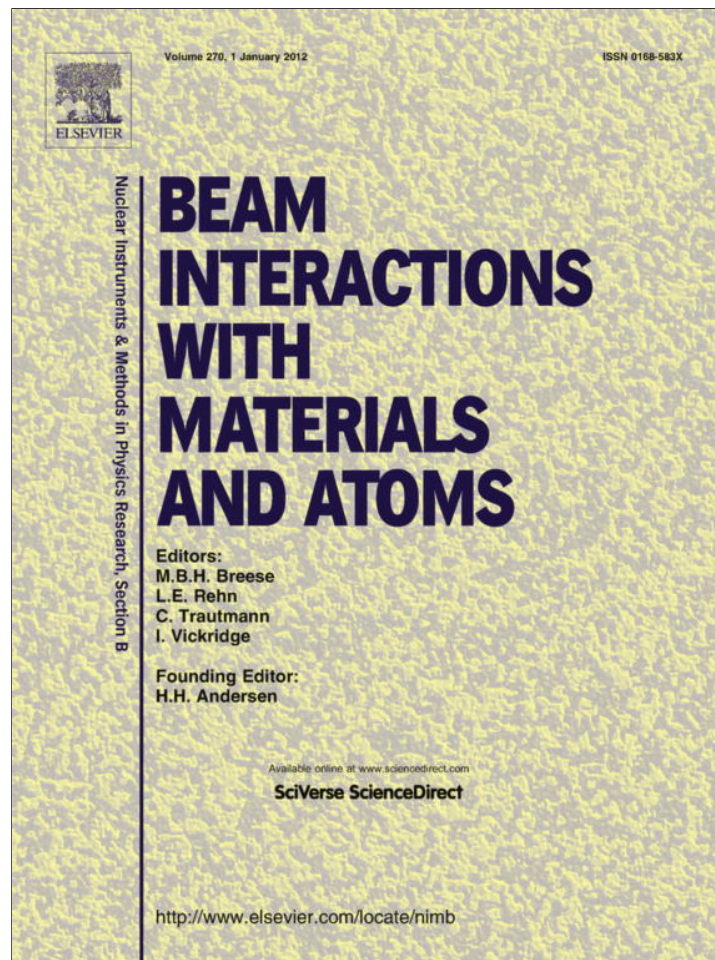


Provided for non-commercial research and education use.
Not for reproduction, distribution or commercial use.



(This is a sample cover image for this issue. The actual cover is not yet available at this time.)

This article appeared in a journal published by Elsevier. The attached copy is furnished to the author for internal non-commercial research and education use, including for instruction at the authors institution and sharing with colleagues.

Other uses, including reproduction and distribution, or selling or licensing copies, or posting to personal, institutional or third party websites are prohibited.

In most cases authors are permitted to post their version of the article (e.g. in Word or Tex form) to their personal website or institutional repository. Authors requiring further information regarding Elsevier's archiving and manuscript policies are encouraged to visit:

<http://www.elsevier.com/copyright>



Contents lists available at SciVerse ScienceDirect

Nuclear Instruments and Methods in Physics Research B

journal homepage: www.elsevier.com/locate/nimb

On the molecular effect in hydrogen molecular ions penetration through thin films

E. Marenkov^{a,*}, V. Kurnaev^a, A. Lasa^b, K. Nordlund^b^a National Research Nuclear University MEPhI, 31, Kashirskoe sh., 115409 Moscow, Russia^b Association Euratom-TEKES, Department of Physics, P.O. Box 43, FI-00014, University of Helsinki, Finland

ARTICLE INFO

Article history:

Received 16 May 2012

Received in revised form 5 July 2012

Available online 16 July 2012

Keywords:

Molecular ions

Carbon films

Stopping power

Electronic straggling

ABSTRACT

Penetration of low energy (2–12 keV) hydrogen molecular ions (H_2^+) and single protons through thin (40 Å) carbon films is simulated using molecular dynamic approach. It is shown that the width of energy loss spectra for the case of H_2^+ penetration is larger than that for H^+ spectra (a “molecular effect”) as it was previously observed in experiments [1]. This is explained by the molecular ions dissociation in the first few monolayers of the target. A simple semi-analytical model accounting for the molecular effect is provided. Results of simulations are compared with experiments.

© 2012 Elsevier B.V. All rights reserved.

1. Introduction

The study of ion and atomic cluster beams interaction with solid targets has been a topic of interest for many years due to both practical and fundamental reasons. Using cluster beams it is possible to create material coatings with unique properties, and the response of a material to cluster impacts is an important tool in surface analysis [2]. Both experimental and theoretical studies show that the effect of a cluster impact on solids is often different from just a sum of single atoms interaction with the solid. For example, it was shown in [3] that the sputtering yield per atom is higher for molecular ions than for individual atoms; the straggling of the depth distribution in a case of gold atom clusters bombarding copper is an increasing function of the cluster size [4], and the sputtering of atoms from surfaces by cluster impacts behaves differently from what is expected in the classical single-atom stopping theory [5].

Molecular ions consisting of two or three constituents are a limiting case of large clusters. They demonstrate a similar nonlinear behaviour comparing to single atom–solid interactions. For example it was observed that bombardment of GaN films with Be_2 ion beams causes enhanced level of implantation-produced lattice disorder in the sample compared to single Be ions bombardment, while the energy per particle remains the same (0.5 MeV) in both cases [6]. Similar nonlinear effects in bombardment with single and molecular ions was studied in [7,8] for particles of MeV energies. The smaller size of molecular ions compared to clusters allows a more detailed study of these effects.

Experiments described in [9] have shown that the energy loss spectra for H_2^+ and H_3^+ ions penetrating through thin (25–70 Å) carbon films are broader than those for single protons (“a molecular effect”). The authors suggested that the reason for such broadening is Coulomb repulsion between protons being the parts of the impinging ion causing the ion dissociation and changing the energy of protons after it. As the energies of the penetrating particles are small and the films used in the experiments are very thin, classical molecular dynamic (MD) method [10] looks like a suitable tool to reproduce the experimental results. In this work we present results of such modelling and suggest a semi-analytical model describing qualitatively well the peaks broadening.

2. Modelling

Simulations were carried out using the PARCAS code [11–13]. The Brenner potential [14] was used to describe all kinds of elastic C–H interactions. It is known that for protons with energies of about 1–10 keV energy loss is primarily defined by electronic (non-elastic) energy losses [15]. The average electronic stopping was obtained from SRIM [16], whereas the classical Lindhard’s model was used to describe the straggling of the electronic stopping of protons in the film [17,18]. Since the low-energy stopping in SRIM is based on the Lindhard model [15], this gives a consistent description of both the average stopping and its straggling.

We note that classical MD simulations do not include variation of the charge state of particles while they are penetrating through the solid. The Brenner potential used is fitted for interactions of neutral hydrogen atoms with each other and with carbon atoms. Therefore, it is more accurate to speak about simulation of H_2 bombardment rather than H_2^+ . However, at ion energies below the

* Corresponding author.

E-mail address: edmarenkov@gmail.com (E. Marenkov).

Fermi velocity of electrons in the solid, an ionic projectile neutralises within the first few monolayers when penetrating through a solid [19]. The remain of its pass in the solid the projectile moves within the Born–Oppenheimer approximation, i.e. its energy at any instant of time is described as if it were on a static atom position. Due to its nature as a bond-order potential [14,20], the Brenner potential should at least in principle describe the energy of the penetrating atoms in any configuration. Hence we expect results of the simulations to be suitable for describing the experimental findings. As for inelastic interactions, the Lindhard's model takes into account the charge state variations.

The following procedure has been used to obtain a film with desired properties. At the first stage, a diamond-like graphite lattice (the simulation cell sizes $62 \times 61 \times 40 \text{ \AA}$, consisting of about 35000 atoms) was heated up to 6000 K and kept at this temperature for 2 ps. After the lattice was melted in this way, the cell was then cooled down to 300 K. During the whole stage periodic boundary conditions were held and the pressure was kept to be 130 GPa. To obtain a fully equilibrated structure one should in principle keep the cooling rate as low as possible. Unfortunately, typical MD simulation timescales do not exceed several nanoseconds. Thus even the slowest cooling rates in MD simulations are still incredibly fast in “real” time. To be sure that the chosen cooling rate is sufficiently low for obtaining an equilibrated structure, different cooling rates were used and the average potential energy E_p was monitored in every case. The dependence of E_p on the cooling rate t_{rate} is shown in Fig. 1 (markers corresponding to obtained values are connected with lines to guide an eye). One sees that $|E_p|$ decreases at higher t_{rate} but becomes approximately constant at the chosen $t_{\text{rate}} \approx 10^{-4} \text{ K/fs}$.

At the second stage, the desired pressure was 0 Pa and the structure obtained at the previous stage was relaxed to this pressure until equilibrium was reached. During the relaxation, the pressure was controlled only along the z axis. Periodic boundary conditions were still used at this stage. At the third stage, a similar relaxation was repeated but the pressure was controlled along all three axes. Finally, two surfaces perpendicular to the z axis were opened (periodic conditions were left only for the x and y axes). After that another short relaxation was performed. As a result, a film with the thickness 42 \AA , the density 1.9 g/cm^3 and the ratio $sp^3/sp^2 \sim 0.5$ was obtained. These characteristics correspond to one of the films used in experiments (the thickness 40 \AA , the density $2.0 \pm 0.2 \text{ g/cm}^3$). However, one cannot expect the simulated film to be a complete representation of the experimental one due to many idealizations MD unavoidably involves.

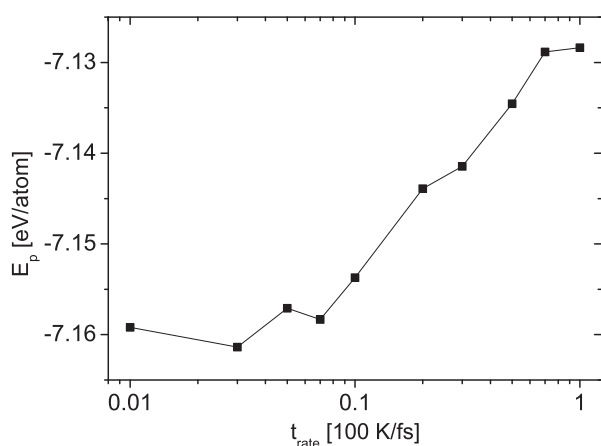


Fig. 1. The average potential energy E_p at the end of quenching against the cooling rate t_{rate} . Markers corresponding to simulated values are connected with lines to guide an eye.

Bombardment of the simulated film was carried out like follows. For the case of H^+ bombardment, the projectile position was chosen randomly above the surface and the velocity of the projectile defined by its energy was directed perpendicular to the surface (i.e. along z direction). For the case of molecular ions penetration, the middle of the molecular axis was situated randomly above the surface in the same way, and the molecular axis orientation was chosen randomly. The distance between H atoms in a molecule was chosen to be 0.73 \AA , which is the equilibrium distance in the potential used. The velocities corresponding in magnitude to the nuclei energies were oriented perpendicular to the film surface. To obtain an energy loss spectrum, about of 5000 impacts were simulated for each case. The maximum allowed time step (PARCAS uses an adaptive time step algorithm to optimize calculations) was set to be 0.01 fs which is much less than characteristic time scales in the problem. Due to rounding errors energy drift is practically unavoidable during MD simulations. In the simulations the maximum energy drift was about of 10 meV/atom which is negligible comparing to the energies of interest.

3. Results and discussion

An example of an energy loss spectrum for H^+ with the initial energy $E_0 = 3860 \text{ eV}$ transmission through the foil is shown in Fig. 2. The markers indicate experimental results taken from [1], the solid line is the energy loss spectrum simulated with PARCAS with electronic energy loss straggling, and the dashed line is the simulated spectrum without electronic straggling. It is clear from this figure that electronic straggling gives dominating contribution in the peak half-width. A shift of the simulated peak to higher energies compared to the experimental values can be explained by a difference in the foil thickness.

A comparison of energy loss spectra for H^+ and H_2^+ penetration is shown in Fig. 3. One notices that the width of the simulated in MD H_2^+ peak (dashed line) is greater than that for the H^+ peak (solid line). It means that we can see the molecular effect in MD simulations.

The origin of the peak broadening can be understood from Fig. 4 where temporal energy dependences are shown for two hydrogen atoms forming a molecule at the beginning. The initial energy was $E_0 = 3860 \text{ eV/atom}$ and the molecular axis was oriented along z direction, i.e. perpendicular to the surface. One notices that for a short time after penetration through the surface (from t_a to t_b in Fig. 4) both atoms lose the energy in a similar way, but then (from t_b to t_c) one starts to gain energy while the other one loses it. This

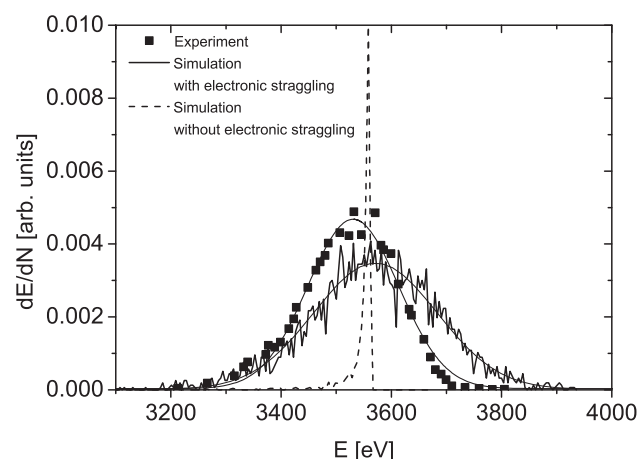


Fig. 2. Energy loss spectra for H^+ transmission through the carbon film. The projectile energy is $E_0 = 3860 \text{ eV}$. Markers are experimental results taken from [1].

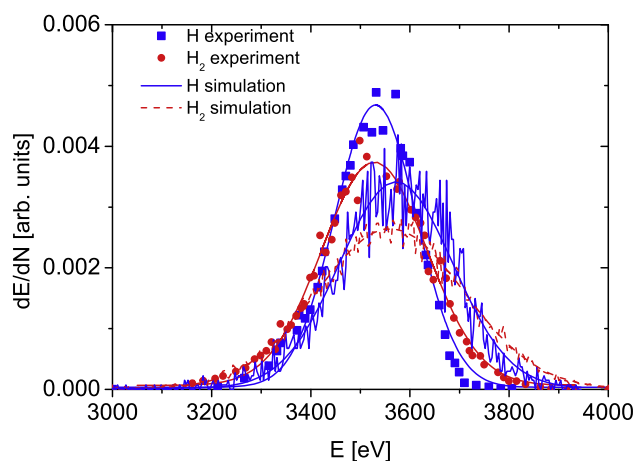


Fig. 3. Comparison of H^+ and H_2^+ spectra for the projectile energy $E_0 = 3860$ eV/nucleus.

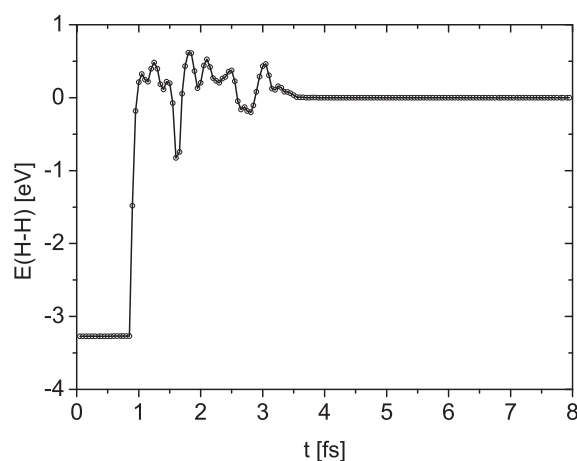


Fig. 5. The interaction energy of two H atoms forming a molecule for the same event as in Fig. 4.

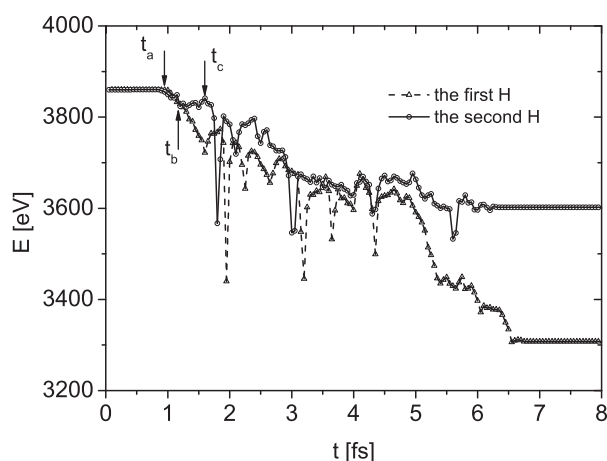


Fig. 4. The temporal energy dependence for H_2^+ constituents. The initial energy is $E_0 = 3860$ eV/nucleus. The molecule axis is perpendicular to the surface.

energy separation lasts for less than one fs, after which the atoms lose the energy independently. One can say that the situation is similar to single ion transmission, but with the initial energy straggled within a range about 100 eV around E_0 . It is clear that in this case, the full width at half maximum (FWHM) of the energy loss spectrum should be greater than it is for the case of actual single ion penetration with all the ions having the same energy E_0 .

The reason for the energy straggling occurs after the molecule has crossed the surface is the molecule dissociation resulting in its fragments getting an additional energy of order of the binding energy E_b (in center of mass system of reference – CMR). Though this value is about only several eV and seems to be much smaller compared to the molecular energy E_0 , it can be shown easily that in the laboratory frame of reference (LFR) the energies of two H atoms after the dissociation are

$$E'_{1,2} = E_0 \pm 2\sqrt{E_0 E_b} \cos \phi \quad (1)$$

where ϕ is the angle between the molecular axis and z direction [21]. Thus the energy difference in the LFR between two hydrogen atoms is about $4\sqrt{E_b E_0}$, which is a significant value.

The process of the molecule breaking down is demonstrated in Figs. 5 and 6 where dependences of the H–H interaction energy (E_{H-H}) and the distance between the fragments r_{H-H} on time are shown (other parameters are the same as in Fig. 4). One notices that the interaction energy starts to increase even before the

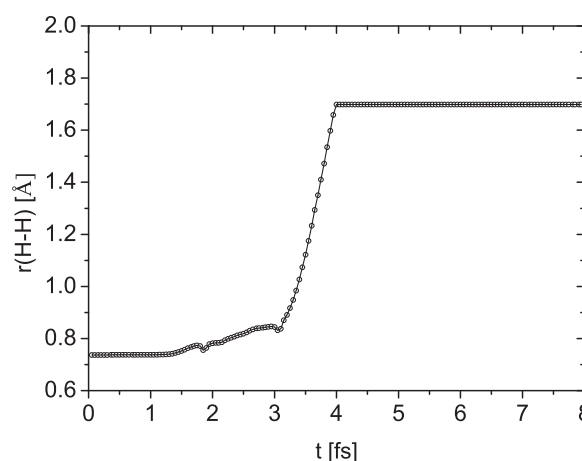


Fig. 6. The distance between the H atoms, for the same event as in Fig. 5.

molecule impact on the surface and becomes positive shortly after that, forcing atoms to repel from each other and r_{H-H} to increase until it becomes larger than the cut-off radius used in the Brenner potential for H–H interaction. From this moment on the hydrogen atoms move through the solid independently.

The cause of the molecular dissociation can be seen directly from the potential used. Indeed, the binding energy of H–H bond is given by expression [14]:

$$E_b = \sum_i \sum_{j>i} [V_R(r_{ij}) - \bar{B}_{ij} V_A(r_{ij})]$$

where the repulsive and attractive pair terms V_R and V_A depend on the distance between hydrogen atoms, while the bond-order term is affected by positions of surrounding carbon atoms. The explicit expression for \bar{B}_{ij} shows that if the distance between a carbon atom and a hydrogen is small enough ($\lesssim 0.5$ Å) the bond-order term \bar{B}_{ij} becomes very small and the repulsive term dominates, making the hydrogen atoms repel from each other. Physically this corresponds to weakening of the H–H bond caused by interaction between the molecule electrons and the valence electrons of the target.

In order to get a quantitative estimation of the peak broadening caused by molecular effect, we plotted FWHM ($\equiv \Delta E_{1/2}$) dependences on the initial energy per atom, E_0 . Results of the calculations along with experimental data are presented in Fig. 7 where

values of $\Delta E_{1/2}/\sqrt{E_0}$ are plotted against E_0 . Full markers represent the experimental results taken from [1], while the hollow ones are obtained by computer simulations. One notices that simulated $\Delta E_{1/2}$ are approximately 40% larger than the experimental values. However, recalling that we do not expect the simulated film structure to be a complete replica of the experimental one, we conclude that agreement between experimental and simulated results for H^+ penetration is satisfactory.

Another deviation of the experimental data from the results of calculations is the behaviour of $\Delta E_{1/2}$ with increase of E_0 . As one sees from Fig. 7, the experimental data are well approximated by constant values, namely $\Delta E_{1/2} = 2.7\sqrt{E_0}$ for H^+ penetration and $\Delta E_{1/2} = 3.3\sqrt{E_0}$ for H_2^+ . Fitting of $\Delta E_{1/2}$ for H^+ PARCAS results (the solid line approximating the hollow squares in the picture) gives $\Delta E_{1/2} \sim E_0^{0.27}$. However, the number of the experimental points is too small to establish precisely dependence of $\Delta E_{1/2}$ on E_0 , especially if we take into account the magnitude of possible experimental errors. Also it was shown in [22] that the exact kind of $\Delta E_{1/2}(E_0)$ behaviour is affected by details of elastic and inelastic energy losses variation with the energy, which are influenced by the target structure and, therefore, can be treated theoretically only approximately.

To verify the results of MD simulation for single protons penetration we also performed SRIM simulations of protons penetration through a carbon layer of 42 Å thickness (the dashed line with circles in Fig. 7). One sees that as it was for MD results, $\Delta E_{1/2}/\sqrt{E_0}$ does not remain constant but decreases when E_0 increases, in agreement with MD simulations.

Unfortunately, the difference in experimental and simulated results for single protons penetration makes direct comparison of the FWHM for H_2^+ transmission unreasonable. To do so, we suggest a simple semi-analytical approach which allows to estimate the peak broadening due to the molecular effect. It is known that for single ions penetration the energy loss spectra have Gaussian shape:

$$\frac{dN}{dE} \equiv f(E) = \exp\left(-\frac{(E - E_m)^2}{2b^2}\right)$$

where both E_m and b depend on the initial energy E_0 . If an amount of protons getting after the ion dissociation an additional energy E' is $dN' = g(E')dE'$ the energy distribution of transmitted particles is

$$\frac{dN}{dE} = \int_{-E_1}^{E_1} f(E, E_0 + E')g(E')dE' \quad (2)$$

where $E_1 = 2\sqrt{E_0\delta E/2}$ is the maximum kinetic energy a fragment can get in the LFR system and $\delta E/2$ is its energy in the CMR. (We

omit all normalisation constants as they do not affect the FWHM.) It is assumed in this equation that the molecular ions dissociate immediately after crossing the surface and the constituents move completely separated from this moment on.

An exact value of δE is defined by details of dissociation mechanism and is difficult to specify precisely. One can say only that this value corresponds to the energy of an antibonding state the molecular ion (or hydrogen) occupied just after it got close to the surface. For example, it was suggested in [21], that when a hydrogen molecular ion approaches the surface it is neutralised quickly either into ground state or into an excited state. If the latter is antibonding its energy is δE . If it is not, subsequent collisions will provide the opportunity for electronic, vibrational and rotational excitation, which may lead to dissociation. So we suggest that δE is the energy of an antibonding state the molecular ion is most probably get into during dissociation process.

It follows from a simple kinematic consideration that if both ion fragments have the same energy in the CMR system and their angular distribution is isotropic in it, their energy distribution in the LFR is uniform, i.e. we have $g(E') = 1$ (see, e.g. [23]; the normalisation constant is left out). The angular distribution in the LFR system is not uniform. However, the maximum angle θ_m between the center of mass velocity V (in the LFR system) and the fragment velocity v_0 (in the C system) is defined as $\sin \theta_m = v_0/V$ and therefore is very small (i.e. the fragments move almost in the same direction as the ion was before disintegration). Thus, we can neglect these variations and assume that all the fragments move perpendicular to the target surface.

Fitting of $\Delta E_{1/2}(E_0)$ and $E_m(E_0)$ dependences based on the results of PARCAS simulations for H^+ penetration gives $b = 11E_0^{0.27}$ eV (the solid line in Fig. 7) and $E_m = 0.98E_0 - 209.6$ eV. Using these functions to calculate dN/dE from (2), we find that the best fit of simulated results is obtained if $\delta E = 4.75$ eV (dashed-dotted line in Fig. 7).

The same method can be applied to estimate a value of δE for H_2^+ from the experimental data. Using the same function for $E_m(E_0)$ but taking b to be proportional to $\sqrt{E_0}$, $b = 1.14\sqrt{E_0}$, we find that to obtain $\Delta E_{1/2}/\sqrt{E_0} = 3.3$ eV $^{-1/2}$ one needs to take $\delta E = 0.7$ eV. This result agrees with values obtained in [21] (0.5–1 eV) from simulations of scattering of H_2^+ from W and Ni surfaces. Therefore, one can say that the difference between the peak broadening due to the molecular effect in experimental and simulated values is primarily caused by the difference in energies of antibonding states for H_2 and H_2^+ .

4. Conclusions

We used the molecular dynamic simulation method to calculate single protons and hydrogen ions penetration through thin carbon films. All kinds of elastic C–H interactions were described using the Brenner potential, while the classical Lindhard's model was employed to account for inelastic energy loss. We have seen that straggling of electronic energy loss gives the main contribution in the peaks width for single protons penetration. The half-width of the energy loss spectra peaks for transmitted protons are in reasonable agreement with the experimental results.

We see that the widths of simulated energy loss spectra for H_2^+ are larger than those for H^+ in agreement with experimental findings. Analysis of temporal dependences of the kinetic energy of transmitting particles shows that the origin of the peaks broadening is in molecular ions dissociation happening as only an ion approaches the target surface. After the dissociation the ion fragments get an additional energy of order of several eV in the center-of-mass system of reference. This energy, however,

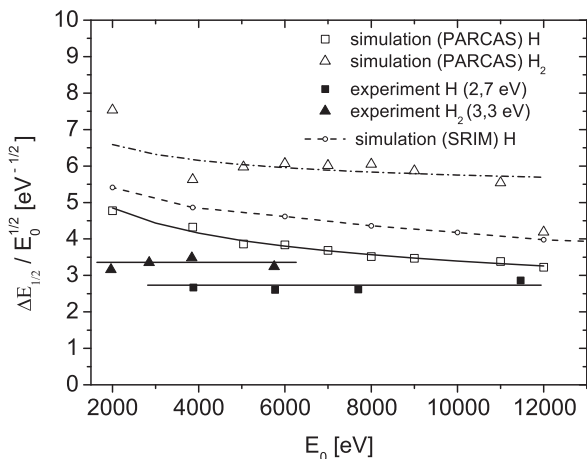


Fig. 7. Experimental and simulated dependences of FWHM on E_0 . Full markers represent the experimental results taken from [1].

corresponds to sufficient energy straggling of the fragments in the laboratory system, which causes the peak broadening.

A simple qualitative model allowing to obtain the energy loss distribution of transmitted particles in case of H_2^+ from known distribution of H^+ is proposed. The half-width of the energy loss spectra depends on the energy the fragments get during the dissociation process, and cannot be specified precisely. It can be suggested that this energy should be of order of the energy of anti-bonding orbitals for the ion.

Acknowledgements

This work was partially supported by Russian Ministry of Education and Science (Grant “FZP-kadry 14.740.11.1171”) and by Association EURATOM-Tekes. Grants of computer time from CSC – IT Center for Science in Espoo, Finland, are also gratefully acknowledged.

References

- [1] E.A. Gridneva, N.N. Koborov, V.A. Kurnaev, N.N. Trifonov, JETP Lett. 1 (2003) 15–17.
- [2] D. Jacquet, Y. Le Beyec, Cluster impacts on solids, Nucl. Instr. Meth. Phys. Res. B 193 (1–4) (2002) 227–239.
- [3] H.H. Andersen, H.L. Bay, Nonlinear effects in heavy-ion sputtering, J. Appl. Phys. 45 (2) (1974) 953–954.
- [4] J. Peltola, K. Nordlund, Heat spike effect on the straggling of cluster implants, Phys. Rev. B 68 (2003) 035419.
- [5] J. Samela, K. Nordlund, Origin of nonlinear sputtering during nanocluster bombardment of metals, Phys. Rev. B 76 (2007) 125434.
- [6] S.O. Kucheyev, J.S. Williams, A.I. Titov, G. Li, C. Jagdish, Effect of the density of collision cascades on implantation damage in gan, Appl. Phys. Lett. 78 (12) (2001) 2694.
- [7] P.A. Karaseov, A.Yu. Azarov, A.I. Titov, S.O. Kucheyev, Density of displacement cascades for cluster ions: an algorithm of calculation and the influence on damage formation in zno and gan, Semiconductors 43 (2009) 691.
- [8] A.I. Titov, S.O. Kucheyev, V.S. Belyakov, A.Yu. Azarov, Damage buildup in si under bombardment with mev heavy atomic and molecular ions, J. Appl. Phys. 90 (8) (2001) 3867–3872.
- [9] E.A. Gridneva, V.A. Kurnaev, N.N. Trifonov, Molecular effect influence on energy spectrum width of hydrogen ions at small-angle scattering, Bulletin of the Russian Academy of Sciences: Physics 70 (6) (2006) 957–960.
- [10] M.P. Allen, D.J. Tildesley, Computer Simulation of Liquids, Oxford University Press, Oxford, England, 1989.
- [11] K. Nordlund, M. Ghaly, R.S. Averback, M. Caturla, T. Diaz de la Rubia, J. Tarus, Defect production in collision cascades in elemental semiconductors and fcc metals, Phys. Rev. B 57 (13) (1998) 7556–7570.
- [12] K. Nordlund, Molecular dynamics simulation of ion ranges in the 1–100 keV energy range, Comput. Mater. Sci. 3 (1995) 448.
- [13] M. Ghaly, K. Nordlund, R.S. Averback, Molecular dynamics investigations of surface damage produced by keV self-bombardment of solids, Phil. Mag. A 79 (4) (1999) 795.
- [14] D.W. Brenner, Empirical potential for hydrocarbons for use in simulating the chemical vapor deposition of diamond films, Phys. Rev. B 42 (15) (1990) 9458–9471.
- [15] J.F. Ziegler, J.P. Biersack, U. Littmark, The Stopping and Range of Ions in Matter, Pergamon, New York, 1985.
- [16] J.F. Ziegler, SRIM-2003 Software Package, available online at: <<http://www.srim.org>>.
- [17] J. Lindhard, M. Scharff, H. Schiott, Range concepts and heavy ion ranges, Mat. Fys. Medd. Dan. Vid. Selsk 33(14) (1963).
- [18] A. Lukkainen, M. Hautala, Calculation of h^+ ranges and h^+ range straggling in the energy region 1–1000 keV, Radiat. Effects 59 (1982) 113–116.
- [19] J. Burgdorfer, F. Meyer, Above-surface neutralization of highly charged ions: the formation of hollow atoms, Phys. Scr. T46 (1993) 225.
- [20] J. Tersoff, Empirical interatomic potential for silicon with improved elastic properties, Phys. Rev. B 38 (1988) 9902.
- [21] W. Heiland, U. Seitat, E. Taglauer, Scattering of molecular and atomic hydrogen ions from single-crystal surfaces, Phys. Rev. B 19 (4) (1979) 1977–1982.
- [22] N.N. Koborov, A.I. Kuzovlev, V.A. Kurnaev, V.S. Remizovich, N.N. Trifonov, Energy distribution of particles transmitted through free foils at oblique incidence, Nucl. Instr. and Meth. B 129 (1997) 5–10.
- [23] E. Lifshitz, L. Landau, Mechanics, Course of Theoretical Physics. Butterworth-Heinemann, Oxford, UK, 1976.